



**University of
Zurich**^{UZH}

**Zurich Open Repository and
Archive**

University of Zurich
Main Library
Strickhofstrasse 39
CH-8057 Zurich
www.zora.uzh.ch

Year: 2012

A petunia ABC protein controls strigolactone-dependent symbiotic signalling and branching

Kretzschmar, Tobias; Kohlen, Wouter; Sasse, Joelle; Borghi, Lorenzo; Schlegel, Markus; Bachelier, Julien B; Reinhardt, Didier; Bours, Ralph; Bouwmeester, Harro J; Martinoia, Enrico

Abstract: Strigolactones were originally identified as stimulators of the germination of root-parasitic weeds that pose a serious threat to resource-limited agriculture. They are mostly exuded from roots and function as signalling compounds in the initiation of arbuscular mycorrhizae, which are plant-fungus symbionts with a global effect on carbon and phosphate cycling. Recently, strigolactones were established to be phytohormones that regulate plant shoot architecture by inhibiting the outgrowth of axillary buds. Despite their importance, it is not known how strigolactones are transported. ATP-binding cassette (ABC) transporters, however, are known to have functions in phytohormone translocation. Here we show that the *Petunia hybrida* ABC transporter PDR1 has a key role in regulating the development of arbuscular mycorrhizae and axillary branches, by functioning as a cellular strigolactone exporter. *P. hybrida* *pdr1* mutants are defective in strigolactone exudation from their roots, resulting in reduced symbiotic interactions. Above ground, *pdr1* mutants have an enhanced branching phenotype, which is indicative of impaired strigolactone allocation. Overexpression of *Petunia axillaris* PDR1 in *Arabidopsis thaliana* results in increased tolerance to high concentrations of a synthetic strigolactone, consistent with increased export of strigolactones from the roots. PDR1 is the first known component in strigolactone transport, providing new opportunities for investigating and manipulating strigolactone-dependent processes.

DOI: <https://doi.org/10.1038/nature10873>

Posted at the Zurich Open Repository and Archive, University of Zurich

ZORA URL: <https://doi.org/10.5167/uzh-74164>

Journal Article

Accepted Version

Originally published at:

Kretzschmar, Tobias; Kohlen, Wouter; Sasse, Joelle; Borghi, Lorenzo; Schlegel, Markus; Bachelier, Julien B; Reinhardt, Didier; Bours, Ralph; Bouwmeester, Harro J; Martinoia, Enrico (2012). A petunia ABC protein controls strigolactone-dependent symbiotic signalling and branching. *Nature*, 483(7389):341-344. DOI: <https://doi.org/10.1038/nature10873>

A petunia ABC protein controls strigolactone-dependent symbiotic signaling and branching

Tobias Kretzschmar¹, Wouter Kohlen^{2*}, Joelle Sasse^{1*}, Lorenzo Borghi¹, Markus Schlegel¹, Julien B. Bachelier¹, Didier Reinhardt⁴, Ralph Bours², Harro J. Bouwmeester^{2,3} & Enrico Martinoia¹

¹Institute of Plant Biology, University of Zurich, 8008 Zurich, Switzerland

²Laboratory of Plant Physiology, Wageningen University, 6700 AR Wageningen, The Netherlands

³Centre for Biosystems Genomics, P. O. Box 98, 6700 AB Wageningen, The Netherlands

⁴Department of Biology, University Fribourg, 1700 Fribourg, Switzerland

*These authors have contributed equally to this work

Strigolactones were originally identified as germination stimulants of root-parasitic weeds¹ that pose a serious threat to resource-limited agriculture². Primarily they are exuded from roots as signaling compounds involved in the initiation of arbuscular mycorrhiza³, a mutual plant-fungal symbiosis with global impact on carbon and phosphate cycling⁴. Recently they were established as phytohormones that regulate plant shoot architecture by inhibiting the outgrowth of axillary buds^{5,6}. Despite their importance, it is unknown how strigolactones are transported. ATP-binding cassette (ABC) transporters have functions in phytohormone translocation⁷⁻⁹. Here we show that the *Petunia hybrida* ABC transporter PhPDR1 plays a key role in regulating arbuscular mycorrhiza and axillary branch development by functioning as a cellular strigolactone exporter. *Phpdr1* mutants are defective in strigolactone exudation from roots, resulting in reduced symbiotic interactions. Aboveground, *phpdr1* exhibits an enhanced branching phenotype, suggestive of impaired

33 **strigolactone allocation. Over-expression of petunia *PDR1* in *Arabidopsis* results in**
34 **increased tolerance to high exogenous strigolactone concentrations, consistent with**
35 **enhanced export from roots. *PDR1* is the first known component in strigolactone**
36 **transport, opening new routes for investigation and manipulation of strigolactone-**
37 **dependent processes.**

38

39 Strigolactones (SLs) are a new class of carotenoid-derived¹⁰ phytohormones in land
40 plants. Besides their role in shoot branching, SLs are exuded into the rhizosphere under
41 P-limiting conditions⁵ to act as growth stimulants of arbuscular mycorrhizal (AM) fungi³.
42 To identify efflux carriers of AM-promoting factors such as SLs, we designed a
43 degenerate primer approach (Supplementary fig. 2a) to isolate full-size ABCG/PDR
44 transporters of petunia abundant in phosphate-starved or mycorrhizal roots. The rationale
45 to focus on ABCG/PDR-type transporters, with 15 members in *Arabidopsis*¹¹, 23 in rice¹¹
46 and 23 putative members in tomato (Supplementary fig. 3a), was that they i) are plasma
47 membrane proteins often found in roots¹²; ii) are implicated in belowground plant-
48 microbe interactions^{13,14}; iii) have affinities for compounds structurally related to
49 SLs^{8,9,15}. Of six primary candidates only *Petunia hybrida PDR1* (*PhPDR1*) displayed
50 enhanced expression in roots subjected to either phosphate starvation (Fig 1a) or
51 colonization by the AM fungus *Glomus intraradices* (Fig. 1b). Furthermore *PhPDR1*
52 transcript levels increased in response to treatments with the synthetic SL analogue GR24
53 and the auxin analogue 1-naphthaleneacetic acid (NAA) (Fig. 1c). Auxin has been shown
54 to up-regulate SL-biosynthetic genes¹⁶ and to be involved in pre-symbiotic and early
55 mycorrhizal events¹⁷.

56 *PhPDR1* is predicted to encode a full-size ABCG/PDR cluster I protein (GenBank
57 accession: JQ292813, Supplementary fig. 2b-c, Supplementary fig. 3b). The closest
58 *Arabidopsis thaliana* homologue, *AtABCG40/AtPDR12*, transports abscisic acid
59 (ABA)⁹. However, as opposed to *AtABCG40*, *PhPDR1* is not regulated by ABA (Fig. 1c).
60 A 1.8 kb upstream element of *PhPDR1* (GenBank accession: JQ292814) was fused to the
61 *GUS* reporter and stably transformed into the petunia cultivar W115. Belowground
62 *pPhPDR1::GUS* expression was pronounced in individual sub-epidermal cells of lateral
63 roots (Fig. 1d-e). These cells largely overlapped with hypodermal passage cells (HPC)
64 (Fig. 1k-m) that are devoid of suberin and serve as cortical entry points for AM hyphae¹⁸.
65 GUS staining was more prominent in roots grown under phosphate-deficient conditions
66 (Fig. 1f) and in mycorrhizal roots, particularly in regions containing or flanking fully
67 developed AM structures (Fig. 1g-h). These results suggested a role in AM during pre-
68 symbiotic development and during intraradical colonization. For localization the genomic
69 *PDR1* orthologue of the *Petunia hybrida* progenitor *Petunia axillaris*, *PaPDR1* (99.7%
70 amino acid identity to *PhPDR1*, GenBank accession: JQ292812, Supplementary figure
71 2b) was C-terminally fused to *GFP* (*GFP::gPaPDR1*). Transient expression of
72 *GFP::gPaPDR1* in *Arabidopsis* showed that PDR1 localizes to the plasma membrane
73 (Fig. 1i-j), consistent with a role in secretion.

74

75 For functional analysis we screened the transposon line W138 for insertional *pdr1*
76 mutants. A PCR-based DNA library screen of 1,000 individuals led to the identification
77 of a *dTph1* insertion in exon 4 of *PhPDR1* (Supplementary fig. 4a-d), together with a

78 footprint allele causing a frameshift (Supplementary fig. 4e). Insertion of the *dTph1* in the
79 coding region of a gene frequently results in a complete loss-of-function¹⁹.

80 W138-*pdrl* was compared directly to W138 and crossed with W115 for further
81 segregation analysis. Five homozygous *pdrl* mutant (W115xW138-*pdrl*) and wild-type
82 lines (W115xW138) were derived from the F2 generation (Supplementary fig. 4d).
83 Phenotypes co-segregated with the *PhPDR1* mutation and transposon display analysis did
84 not reveal other co-segregating *dTph1* insertions in the W115xW138 lines
85 (Supplementary fig. 4f), suggesting that *dTph1* insertion in *PhPDR1* is responsible for the
86 observed phenotypes. In addition, *PhPDR1* knock-down lines (*phpdrl*-RNAi), created in
87 W115 by use of two independent RNAi constructs (Supplementary fig. 5a-b), exhibited
88 similar phenotypes.

89

90 W138-*pdrl* displayed a significantly reduced ability to accommodate *Gigaspora*
91 *margarita* and *G. intraradices* (Fig 2a), two distantly related AM fungi with different
92 growth strategies⁴. This finding indicated that PDR1 functions as a transporter of a
93 stimulatory molecule involved in symbiosis with diverse AM fungal species. Indeed, root
94 exudates from W138-*pdrl* showed reduced activity to stimulate hyphal branching of *G.*
95 *margarita* in an *in vitro* bioassay (Fig. 2b). As these results suggested an involvement of
96 SLs, W115xW138-*pdrl* root exudates were assessed for their ability to stimulate
97 germination of the root-parasitic weed *Phelipanche ramosa* (Orobanchaceae). As control,
98 root exudates of *dad1* in the petunia cultivar V26 were used. *DAD1* encodes *Carotenoid*
99 *Cleavage Dioxygenase 8 (CCD8)*²⁰, an orthologue of the established SL-biosynthetic
100 genes *RMS1*, *MAX4* and *D10* in pea, *Arabidopsis* and rice, respectively^{5,6}. The

101 germination rate of *P. ramosa* was significantly lower with root exudates of
102 W115xW138-*pdr1* and *dad1* compared to exudates of the corresponding wild types,
103 which induced germination to a similar extent as GR24 (Fig. 2d). Comparable results
104 were obtained with *phpdr1*-RNAi lines (Supplementary figure 5c). When inoculated with
105 *G. intraradices*, W115xW138-*pdr1* lines displayed similarly retarded colonization rates
106 as W138-*pdr1* and *dad1* (Fig. 2c). Despite the delay in AM development, neither
107 W115xW138-*pdr1* nor *dad1* displayed any morphological aberrations in intracellular
108 mycorrhizal structures (Fig. 2e-h). Intraradical hyphae and arbuscules appeared normal,
109 suggesting that the quantitative differences in colonization are due to a decreased number
110 of hyphal penetrations and retarded intraradical expansion of AM fungal colonies, rather
111 than to defects in intracellular fungal development. Thus, the phenotype of *dad1* and
112 *phpdr1* was distinct from AM mutants such as *pam1*²¹, *str1*²² or SYM-pathway mutants⁴
113 that commonly exhibit aberrant AM fungal structures.

114 Detailed analysis of W138 root exudates resulted in the identification of the SL
115 orobanchol (Supplementary figure 6). Orobanchol levels in *phpdr1* root exudates were
116 significantly reduced compared to wild-type plants (Fig. 3a), whereas the levels in root
117 extracts were not affected (Fig. 3b), indicating that *phdr1* is not defective in SL
118 biosynthesis. Orobanchol was detectable neither in root exudates nor in root extracts of
119 *dad1* confirming its supposed defect in SL biosynthesis (Fig. 3a-b). The finding, that only
120 extraradical orobanchol levels were affected in *phdr1*, indicated that PDR1 functions as
121 an SL export carrier.

122 PDR1-dependent SL transport was further explored in a heterologous system by stable
123 and constitutive over-expression of *GFP::gPaPDR1* in *Arabidopsis* Col-0, resulting in

124 *PDR1*-OE lines (Supplementary fig. 7a-b). *Arabidopsis* does not form AM and exudes
125 only minute quantities of SLs²³. When grown on GR24-containing medium, *PDR1*-OE
126 lines proved more tolerant to the deleterious effects of high SL concentrations on root
127 elongation²⁴ than the wild type (Fig. 3c, Supplementary fig. 7c). Direct SL exudation was
128 assessed by quantifying the efflux of pre-loaded ³H-GR24 from roots either incubated at
129 4°C, to monitor passive diffusion, or at 23°C, enabling transporter-mediated efflux. After
130 a period of 1 h *PDR1*-OE roots incubated at 23°C retained significantly less GR24
131 compared to controls at 4°C (Fig. 3d, Supplementary fig. 7d). In agreement with this
132 observation, more GR24 was found in root exudates of *PDR1*-OE lines at 23°C. No
133 significant differences were found for root extracts or root exudates of wild-type or vector
134 control lines in either condition (Fig. 3d). These results together with the observed GR24-
135 resistance phenotype of *PDR1*-OE are best explained with PDR1 acting as an SL
136 exporter.

137 Taken together, our data suggest a role for PDR1 in SL secretion from HPC. We
138 hypothesize that PDR1-mediated SL exudation under low phosphate conditions creates
139 local rhizospheric gradients that guide AM hyphae to HPC, which are susceptible to
140 hyphal penetration (Supplementary fig. 1), thereby initiating AM. The symbiotic
141 phenotype of *phpdr1* and *dad1*, and the induction of *PhPDR1* in colonized root segments
142 suggests that SLs may play an additional role in promoting sustained intercellular root
143 colonization, whereas intracellular stages (*e.g.* arbuscules) develop independently from
144 SLs (Fig. 2e-h).

145 Recently it was demonstrated that SLs inhibit shoot branching^{5,6}. Although some aspects
146 of SL biosynthesis and signaling were unraveled²⁵, information about its mode of

147 transport is scant. SLs are mobile within the xylem sap²³, but it is unknown how they are
148 released from producing cells and whether directed cell-to-cell transport exists. SL
149 biosynthesis is subject to direct negative feedback regulation²⁶. Hence SL biosynthesis
150 needs to be coordinated with export to prevent SL accumulation to levels that would
151 restrict further production. Indeed, *PhPDR1* expression was found to be stimulated by
152 exogenous application of GR24 (Fig. 1c and 4a), suggesting substrate-dependent
153 induction, as previously observed for other *ABCG* subfamily^{9,15} members.

154 Aboveground *PhPDR1* expression was largely confined to stem tissues, particularly the
155 vasculature and nodal tissues adjacent to leaf axils (Fig. 4b, c). However, *PhPDR1*
156 expression was absent from dormant buds (Fig. 4d). This pattern is consistent with a
157 function of PDR1 as an SL transporter. While SLs are xylem-mobile²³, a cellular
158 transport system is required to deliver SL to dormant buds that are not yet connected to
159 the xylem. This scenario is compatible with both current models for SL-dependent
160 branching control²⁷. According to the ‘second messenger model’, SLs are transported into
161 the bud as a second messenger of auxin²⁸, hence cellular transport of SL in the axillary
162 regions would be indispensable. In the ‘auxin transport canalization-based model’ SLs
163 are thought to dampen polar auxin transport, resulting in the accumulation of auxin to
164 levels that inhibit bud outgrowth²⁹. SL could restrict auxin transport systemically and/or
165 locally²⁷. For both models local SL transport capacity near the axils would be in line with
166 the inhibitory role of SL on branching. In W115xW138-*pdr1*, bud outgrowth was
167 initiated sooner (Supplementary fig. 8a) and more vigorously than in the wild type,
168 causing longer branches (Fig. 4e, Supplementary fig. 8e-h) at node three to five. This was
169 also observed in *phpdr1*-RNAi lines (Fig. 4f). *Dad1* initiates branches from all nodes

170 (Supplementary fig. 8d), and though branch elongation is retarded, it eventually produces
171 full branches from every node^{20,30}. At flowering time this results in a phenotype that is
172 more pronounced than in any of the *phpdr1* mutants, which display final branch patterns
173 that differ only marginally from the respective wild types (Supplementary fig. 8b-c,
174 Supplementary table 1). Nevertheless the *phpdr1* branching phenotype appears SL-
175 dependent and related to the *dad1* branching phenotype, as branch elongation in both
176 mutants could be suppressed to near wild-type conditions by exogenous application of
177 GR24 to the leaf axils (Fig. 4 g-h).

178 In conclusion, the identification of PDR1-mediated SL transport contributes to a more
179 comprehensive view of SL modes of action. Understanding the underlying transport
180 mechanisms is crucial for a holistic view of phytohormone function. SL transport has
181 direct impact on phosphate-dependent control of AM levels and on control of shoot
182 branching, where the integration of auxin and SL signaling seems partially achieved
183 through reciprocal transport modulation. The mild branching phenotype of *phpdr1*
184 relative to the SL biosynthetic mutant *dad1*³⁰ suggests that residual transport and/or
185 locally produced SLs may compensate for defective SL transport in the shoot. However,
186 AM development was affected to a similar degree in *phpdr1* and *dad1*, revealing that
187 belowground SL transport and secretion relies primarily on PDR1.

188

189 **Methods summary:**

190 All experiments with exception of transport assays were performed in accordance with
191 established protocols. Detailed methods and associated references can be found online as
192 supplementary information.

193

194 **Acknowledgements:**

195 We kindly thank: C. Gübeli for technical assistance; T. Gerats, S. Hörtensteiner, A.
196 Osbourne, P. Schläpfer and C. Beveridge for comments. This study was funded by the
197 Swiss National Foundation within the NCCR-Plant Survival, the project “ABC
198 transporters involved in signaling” and by The Netherlands Organization for Scientific
199 Research (NWO; VICI grant, 865.06.002 and Equipment grant, 834.08.001 to H.B.). H.B.
200 was co-financed by the Centre for BioSystems Genomics (CBSG).

201

202 **Author contributions:**

203 T.K. wrote the manuscript, designed the project and carried out most of the experiments.
204 W.K. and R.B. carried out the LC-MS/MS analysis and the *P. ramosa* bioassays. J.S.
205 performed qRT analysis and transport. J.S. and M.S. performed branching and GUS
206 trials. L.B. analyzed *PDRI*-OE lines. J.B. sectioned material. D.R. investigated AM
207 morphology. H.B. supervised the analytical part of the project. E.M. conceived and
208 supervised the project. DR, EM, JS, WK and HB assisted in editing.

209

210 **REFERENCE LIST:**

211

- 212 1. Cook, C. E., Whichard, L. P., Turner, B., Wall, M. E. & Egle, G. H. Germination
213 of Witchweed (*Striga lutea* Lour.): Isolation and Properties of a Potent Stimulant.
214 *Science* **154**, 1189-1190 (1966).
- 215 2. Yoder, J. I. & Scholes, J. D. Host plant resistance to parasitic weeds; recent
216 progress and bottlenecks. *Current Opinion in Plant Biology* **13**, 478-484 (2010).
- 217 3. Akiyama, K., Matsuzaki, K.-i. & Hayashi, H. Plant sesquiterpenes induce hyphal
218 branching in arbuscular mycorrhizal fungi. *Nature* **435**, 824-827 (2005).

- 219 4. Parniske, M. Arbuscular mycorrhiza: the mother of plant root endosymbioses. *Nat*
220 *Rev Microbiol* **6**, 763-775 (2008).
- 221 5. Umehara, M. et al. Inhibition of shoot branching by new terpenoid plant
222 hormones. *Nature* **455**, 195-200 (2008).
- 223 6. Gomez-Roldan, V. et al. Strigolactone inhibition of shoot branching. *Nature* **455**,
224 189-194 (2008).
- 225 7. Petrasek, J. & Friml, J. Auxin transport routes in plant development. *Development*
226 **136**, 2675-2688 (2009).
- 227 8. Kuromori, T. et al. ABC transporter AtABCG25 is involved in abscisic acid
228 transport and responses. *Proc Natl Acad Sci U S A* **107**, 2361-2366 (2010).
- 229 9. Kang, J. et al. PDR-type ABC transporter mediates cellular uptake of the
230 phytohormone abscisic acid. *Proc Natl Acad Sci U S A* **107**, 2355-2360 (2010).
- 231 10. Matusova, R. et al. The strigolactone germination stimulants of the plant-parasitic
232 *Striga* and *Orobancha* spp. are derived from the carotenoid pathway. *Plant Physiol*
233 **139**, 920-934 (2005).
- 234 11. Verrier, P. J. et al. Plant ABC proteins--a unified nomenclature and updated
235 inventory. *Trends Plant Sci* **13**, 151-159 (2008).
- 236 12. Moons, A. Transcriptional profiling of the PDR gene family in rice roots in
237 response to plant growth regulators, redox perturbations and weak organic acid
238 stresses. *Planta* **229**, 53-71 (2008).
- 239 13. Badri, D. V. et al. An ABC transporter mutation alters root exudation of
240 phytochemicals that provoke an overhaul of natural soil microbiota. *Plant Physiol*
241 **151**, 2006-2017 (2009).
- 242 14. Sugiyama, A., Shitan, N. & Yazaki, K. Signaling from soybean roots to
243 rhizobium: An ATP-binding cassette-type transporter mediates genistein
244 secretion. *Plant Signal Behav* **3**, 38-40 (2008).
- 245 15. Jasinski, M. et al. A plant plasma membrane ATP binding cassette-type
246 transporter is involved in antifungal terpenoid secretion. *Plant Cell* **13**, 1095-1107
247 (2001).
- 248 16. Hayward, A., Stirnberg, P., Beveridge, C. & Leyser, O. Interactions between
249 auxin and strigolactone in shoot branching control. *Plant Physiol* **151**, 400-412
250 (2009).
- 251 17. Hanlon, M. T. & Coenen, C. Genetic evidence for auxin involvement in
252 arbuscular mycorrhiza initiation. *New Phytologist* **189**, 701-709 (2011).
- 253 18. Sharda, J. N. & Koide, R. T. Can hypodermal passage cell distribution limit root
254 penetration by mycorrhizal fungi? *New Phytologist* **180**, 696-701 (2008).
- 255 19. Koes, R. et al. Targeted gene inactivation in petunia by PCR-based selection of
256 transposon insertion mutants. *Proc Natl Acad Sci U S A* **92**, 8149-8153 (1995).
- 257 20. Snowden, K. C. et al. The Decreased apical dominance1/*Petunia hybrida*
258 CAROTENOID CLEAVAGE DIOXYGENASE8 gene affects branch production
259 and plays a role in leaf senescence, root growth, and flower development. *Plant*
260 *Cell* **17**, 746-759 (2005).
- 261 21. Reddy D M R, S., Schorderet, M., Feller, U. & Reinhardt, D. A petunia mutant
262 affected in intracellular accommodation and morphogenesis of arbuscular
263 mycorrhizal fungi. *Plant J* **51**, 739-750 (2007).

- 264 22. Zhang, Q., Blaylock, L. A. & Harrison, M. J. Two *Medicago truncatula* half-ABC
265 transporters are essential for arbuscule development in arbuscular mycorrhizal
266 symbiosis. *Plant Cell* **22**, 1483-1497 (2010).
- 267 23. Kohlen, W. et al. Strigolactones are transported through the xylem and play a key
268 role in shoot architectural response to phosphate deficiency in nonarbuscular
269 mycorrhizal host *Arabidopsis*. *Plant Physiol* **155**, 974-987 (2011).
- 270 24. Ruyter-Spira, C. et al. Physiological effects of the synthetic strigolactone analog
271 GR24 on root system architecture in *Arabidopsis*: another belowground role for
272 strigolactones? *Plant Physiol* **155**, 721-734 (2011).
- 273 25. Beveridge, C. A. & Kyojuka, J. New genes in the strigolactone-related shoot
274 branching pathway. *Curr Opin Plant Biol* **13**, 34-39 (2010).
- 275 26. Mashiguchi, K. et al. Feedback-regulation of strigolactone biosynthetic genes and
276 strigolactone-regulated genes in *Arabidopsis*. *Biosci Biotechnol Biochem* **73**,
277 2460-2465 (2009).
- 278 27. Domagalska, M. A. & Leyser, O. Signal integration in the control of shoot
279 branching. *Nat Rev Mol Cell Biol* **12**, 211-221 (2011).
- 280 28. Brewer, P. B., Dun, E. A., Ferguson, B. J., Rameau, C. & Beveridge, C. A.
281 Strigolactone Acts Downstream of Auxin to Regulate Bud Outgrowth in Pea and
282 *Arabidopsis*. *Plant Physiol*. **150**, 482-493 (2009).
- 283 29. Crawford, S. et al. Strigolactones enhance competition between shoot branches by
284 dampening auxin transport. *Development* **137**, 2905-2913 (2010).
- 285 30. Napoli, C. Highly Branched Phenotype of the *Petunia dad1-1* Mutant Is Reversed
286 by Grafting. *Plant Physiol* **111**, 27-37 (1996).
- 287
288
289
290
291
292
293
294
295
296
297
298
299
300
301
302
303
304
305
306
307
308
309

310

311 **Figure legends:**

312

313 **Figure 1 | Belowground *PhPDR1* expression and PDR1 localization**

314 **a-c**, qPCR for *PhPDR1* in W115 roots; in presence or absence of phosphate (P) (**a**); 2-4
315 weeks post inoculation (wpi) with *G. intraradices* (**b**); in response to H₂O, GR24, NAA,
316 ABA (**c**); means ± s.e.m. (N = 3). **d-h**, *pPhPDR1::GUS* signal in W115 roots without
317 treatment (E: epidermal cell) (**d-e**); under P-sufficient and P-deficient conditions (**f**); in
318 response to mycorrhization (+MYC = 8 wpi) (**g**) in mycorrhized roots (8 wpi) co-stained
319 with black ink (black arrows; mycorrhized sections) (**h**). Scale bars = 1 mm (e: 0.1 mm).
320 **i-j**, Transient *CaMV 35S::GFP-gPaPDR1* expression in *Arabidopsis* mesophyll
321 protoplasts. GFP- gPaPDR1 signal and corresponding transmission image (**i**) and free
322 GFP signal and transmission image (**j**). Scale bar = 10 µm. **k-m**, *pPhPDR1::GUS* signal
323 co-localization with trypan blue stained root hypodermal passage cells. Magenta GUS
324 stained root section (**k**); additional trypan blue stain of the same sample (**l**) and stained
325 wild-type (**m**). Scale bars = 0.1 mm.

326

327 **Figure 2 | Belowground *phpdr1* phenotypes**

328 **a**, AM colonization of W138 and W138-*pdrl* roots 8 wpi with two AM fungi, means ±
329 s.e.m. (N > 20). **b**, *In vitro* branching response of *G. margarita* 24 h after GR24
330 application (N = 5), root exudates of W138 (N = 17), W138-*pdrl* (N = 36) or 10%
331 acetone (solvent, N = 5), means ± s.e.m.. **c**, Kinetics of *G. intraradices* colonization of
332 W115xW138 (N = 25), W115xW138-*pdrl* (N = 25), V26 (N = 5) *dad1* (N = 5), means
333 ± s.e.m. (p < 0.001 for all time points between mutants and wild-types). **d**, *P. ramosa*
334 germination induced by GR24 (N = 3), root exudates of W115xW138 (WxW WT, N =
335 10), W115xW138-*pdrl* (WxW *pdrl*, N = 10), V26 (N = 4), *dad1* (N = 4) or water (N =
336 4), means ± s.e.m.. **e-h**, *G. intraradices* intracellular AM morphology 4 wpi in
337 W115xW138 (**e**); W115xW138-*pdrl* (**f**); V26 (**g**) and *dad1* (**h**). Scale bars = 20 µm. * =
338 p < 0.05; *** = p < 0.001 in all panels

339

340 **Figure 3 | Orobanchol contents and PDR1-dependent GR24 tolerance and transport**

341 **a-b** Orobanchol in the root exudates (**a**) and extracts (**b**) of *Phpdrl* lines, *dad1* and wild-
342 types (N = 9), means ± s.e.m. **c**, Col-0 and *PDR1*-OE grown on 0, 10, and 25 µM GR24.
343 Scale bar = 1 cm **d**, Export assay of ³H-GR24 preloaded roots of Col-0, vector control
344 (VC) and *PDR1*-OE lines (OE L1-3). Relative ³H-GR24 in the medium (water), root and
345 shoot, after 1 hour incubation at 4°C and 23°C; means ± s.e.m. (N = 8). * = p < 0.05; ***
346 = p < 0.001 in all panels.

347

348 **Figure 4 | Aboveground *PhPDR1* expression and *phpdr1*-related branching**
349 **phenotypes**

350 **a-b**, qPCR for aboveground W115 GR24-treated tissue (**a**) and different organs (**b**);
351 means ± s.e.m. (N = 3). **c-d**, *pPhPDR1::GUS* in W115 at the four-leaf stage (**c**) and a
352 node close-up (**d**) (white arrow: dormant axillary bud). Scale bars: b = 10 mm; d = 1
353 mm. **e-f**, Branch development 41 days post germination (dpg); means ± s.e.m., Branch
354 length for W115xW138 and W115xW138-*pdrl* (N = 110) (**e**) and for W115 and two
355 *Phpdrl*-RNAi lines, R104 (p < 0.001 for node 3-4), and C244 (p < 0.05 for node 3)

356 (N=8) **(f)**. **g-h**, Effects of GR24 (striped) on branch development 34 dpg at node 3-5 for
357 W115xW135 and W115xW138-*pdrl* (N = 24), **(g)** V26 and *dad1* (N = 8) **(h)**; means \pm
358 s.e.m. *=p<0.05;***=p<0.001 in all panels
359
360
361
362
363
364
365
366
367
368
369
370
371
372
373
374
375
376
377
378
379
380
381
382
383
384
385
386
387
388
389
390
391
392
393
394
395
396
397
398
399
400
401

402 **Methods and materials (supplementary online information):**

403 **1 Plant growth conditions**

404 Petunia lines were grown at 16 h light, 60% relative humidity and 25°C in soil (ED 73
405 Einheitserde, Einheitserde Werksverband e.V., Germany) or in clay granules (Oil Dry US
406 Special, Damolin, Switzerland). Clay granules were supplemented once a week with half-
407 strength Hoagland solution. For mycorrhization trials a mix of 40% [v/v] soil, 40% [v/v]
408 clay granules, 10% [v/v] sand and 10% [v/v] mycorrhizal inoculum (AGRAUXINE,
409 France) was used. Seeds were plated on medium containing 2.2 g L⁻¹ MS (Duchefa, The
410 Netherlands) and 15 g L⁻¹ sucrose, supplemented with 9 g L⁻¹ PHYTO AGAR (Duchefa,
411 The Netherlands) at 16 h of light and 25°C. *Arabidopsis thaliana* was grown in vertical
412 plates on medium containing 2.2 g L⁻¹ MS (Duchefa, The Netherlands) and 15 g L⁻¹
413 sucrose, supplemented with 9 g L⁻¹ PHYTO AGAR (Duchefa, The Netherlands) at 16 h
414 light, 60% relative humidity and 21°C. For hormone treatment 14 d old W115 seedlings
415 grown on plate were exposed for 24 h with final concentrations of 1 or 10 µM of the
416 synthetic SL analog GR24 (Chiralix, The Netherlands), 10 µM abscisic acid (ABA) or 25
417 µM 1-naphthaleneacetic acid (NAA). For phosphate starvation 14 d old W115 seedlings
418 were transferred to P-free plates for one week.

419

420 **2 PDR1 cloning strategy**

421 *PDR*-specific 0.5 kb transcripts were amplified from W115 root cDNA five wpi with *G.*
422 *intraradices* with: 5'-mgwatgactctdytkytkggacctcc and 5'-gyttcytytgnccchcchgaatwcc
423 (5' region) or with: 5'-gggwaaracggwgtyagtggwgcw and 5'-ctcatnacaatdgcwgcwgcctctwgc
424 (3' region). Resulting 5' and 3' fragments were aligned and the deduced consensus
425 primers 5'-tattgggacttgaattgtgccgatac and 5'-gctcactaacacccatcagagctgtc were used to
426 amplify putative *PDR* fragments spanning 2.5 kb. 5' and 3' ends of *PhPDR1* were
427 amplified using the SMART-RACE Amplification Kit (Clontech, Takara Bio Company,
428 USA) with 5'RACE 5'-ctcgagtacattttctcggggaccttg, nested 5'RACE 5'-
429 ccatttctctccaacaatggtatcgg, 3'RACE 5'-gtcctcaagagtaggaagcatcactgcg and nested
430 3'RACE 5'-accgaggaccggcttgaactcttgagag. Full length *PhPDR1* cDNA GenBank
431 accession is JQ292813.

432 To obtain the full length genomic sequence of *PDR1* a *Petunia axillaris* BAC library
433 (kind gift of Chris Kuhlemeier, University of Bern) was screened with: 5'-
434 tgccaatccttcatgatgtcagtg and 5'-ccttctctctcctagacagctctgc. *P. axillaris* is a progenitor of
435 the hybrid species *P. hybrida*³¹ and a genomic library for BAC-based cloning was only
436 available for the former. BACs were extracted from candidate clones via the Large
437 Construct Kit (Qiagen, Germany). Full length genomic *PaPDR1* was amplified from BAC
438 with 5'-aattactagtatggagggtggtgaag and 5'-aattgcacgcctatctttctggaaattaaatg cut with *SpeI*
439 and *SphI* and cloned into pUC18-GFP5sp via compatible *NheI* and *SphI* restriction sites
440 for GFP localization studies³². For stable transformation the *CaMV*
441 *35S::GFP::gPaPDR1-terminator* cassette was cloned from pUC18-GFP5sp into
442 pGreenII0179 vector³³ via the following strategy: i) The *CaMV 35S* promoter from native
443 pUC18-GFP5sp was cloned via *XhoI* and *XmaI*. ii) The terminator from the native
444 pUC18-GFP5sp including the upstream *SphI* site was cut with *NheI* and *SacI* and inserted
445 into *CaMV 35S* -pGreenII0179 via compatible *XbaI* and *SacI* sites. iii) *GFP::gPaPDR1*
446 was cut and cloned via *XmaI* and *SphI*. 9 kb of the genomic *PaPDR1* locus, including
447 upstream and downstream sequence, are submitted with GenBank under accession
448 JQ292812.

449

450 **3 *PhPDR1* promoter GUS construct and GUS staining assay**

451 A 1.8 kb *PhPDR1* promoter fragment was amplified using the Genome Walker Universal
452 Kit (Clontech, Takara Bio Company, USA) with 5`-agttggaagtttctcaagtgcagccca and the
453 nested 5`-ccctaaagagttctcaccaccctccat (GenBank accession JQ292814). The fragment
454 was cloned into the pGEM-T-Easy vector system (Promega, USA), reamplified with 5'-
455 catgaagcttgcaccagaagaagattagc and 5'-tcgatctagacacattaagaggaaagtaggtac and cloned
456 into the pGPTV-Bar³⁴ vector system via *HindIII* and *XbaI*. Of the original T0
457 transformants eight lines were selected for further analysis. Segregating T1 individuals of
458 all eight lines displayed comparable belowground and aboveground expression patterns at
459 different developmental stages. Two of these lines were chosen for the in depth analysis
460 presented in this work and all data presented was confirmed in both lines.
461 GUS-staining trials were performed as described previously³⁵. After staining, samples
462 were cleared for 24 h in 10% [w/v] KOH and stored in 70% [v/v] ethanol. For analysis of

463 hypodermal passage cells, 5-bromo-6-chloro-3-indolyl β -D-glucuronide
464 cyclohexylammonium salt was used for GUS staining and samples were cleared for 24 h
465 in 10% [w/v] KOH before staining with trypan blue as described¹⁸.

466

467 **4 *PhPDRI* RNA interference constructs**

468 Silencing of *PhPDRI*-specific transcripts was performed with the pKANNIBAL vector
469 system³⁶. Two constructs were designed, one targeting a highly variable region within the
470 nucleotide binding domain 2 (NBD2) of *PhPDRI* (C-construct) and one targeting a part
471 of the 3' end and the 3'UTR of *PhPDRI* (R-construct). The 148 bp C-fragment
472 (ggaacgcaagcaaaaggggtgaggtattgaactatcttcgcttgaaagagctctctgaaaaaggaaatgatgttcggcgaa
473 gtgcatctccaggcaatgtcctcaagagtaggaagcatcactgcggtgattgagcaagag) was amplified from
474 W115 cDNA with 5'-cgatggatcctcgagggaacgcaagcaaaaggg, containing *Bam*HI and *Xho*I
475 restriction sites and 5'-cgatatcgatggtaccctcttgcctcaaatcagccgcagtga containing *Cla*I and
476 *Kpn*I sites. The 411 bp R-fragment (gacattataggactaattgcctcacaattggagacatacaagacag
477 acttgacacaaatgagacagtggacaattcatagagaattctttgattcaaacatgattttgtgggatattgctctcattctgtt
478 gggattctgttcttttctctcattttgcattttcaattaaacatttaattccagaaaagataggttggtccagggtatacatgaaa
479 agagcgtttatcaagatatgtgtatattaggataataataatcttcttttctctttttactattgtggtttctcaagtttgaataga
480 tagaaccaaaagtctgtactctgtatttaagaacaactttgtacacattgttatgtattggagaagttatgagtatctttg) was
481 amplified with 5'-cgatggatcctcgagacattataggactaattgcc, containing *Bam*HI and *Xho*I
482 restriction sites and 5'-cgatatcgatggtaccaaaagatactcataacttctcc containing *Cla*I and *Kpn*I
483 sites. The resulting amplicons were cloned in sense and antisense direction in the two
484 multiple cloning sites of pKANNIBAL. The pKANNIBAL RNAi cassette was excised
485 from the vector backbone via *Not*I and transferred into the binary pGreenII0229 vector³³.
486 After stable transformation of W115 the extent of down-regulation was estimated via
487 semi-quantitative PCR or RT-PCR.

488

489 **5 Plant transformation**

490 W115 was transformed as described³⁷. Construct insertion was confirmed via PCR on
491 genomic DNA with 5'-acggtccacatgccggtatatac gatg and 5'-gatggcattgtaggagccaccttc,
492 targeting the CaMV35S promoter, or with 5'-gaattgatcagcgttggtgggaaagc and 5'-
493 ggtaatgcgaggtacggttaggagttg, targeting the GUS gene.

494 Transient transformation of *Arabidopsis thaliana* Col-0 protoplasts was performed as
495 described previously³². *Arabidopsis* plants were stably transformed as described³⁸. T0
496 generation was selected for hygromycin resistance. Plants of the T1 generation were
497 tested for hygromycin resistance and GFP expression.

498

499 **6 Screening approach to identify transposon insertions in *PhPDR1***

500 A 3D-gDNA library (kind gift from Tom Gerats, Radboud University, Nijmegen)
501 representing 10x10x10 (1,000) W138 individuals was screened for *dTph1* insertions in
502 *PhPDR1* via a PCR-based method³⁹. The entire genomic region of *PhPDR1* was scanned
503 in contiguous steps covering less than 1 kb, using the *dTph1*-specific primer 5'-
504 gaattcgtctccgccctg and a variety of ³³P-labeled gene-specific primers. The primer 5'-
505 ccatttcgtctccaacaatggtatcgg yielded a positive result. Homozygosity PCRs were
506 performed with the transposon flanking primers: 5'-tgccaatccttcgatgagtcagtg and 5'-
507 ccttctctctcctagacagctctgc. Homozygous *dTph1* insertion alleles were furthermore crossed
508 into W115, the progeny selfed and the resulting offspring tested for homozygosity with
509 the above mentioned primers. Transposon display analysis utilizing six W115xW138 and
510 five W115xW138-*pdr1* lines was performed as described⁴⁰.

511

512 **7 Mycorrhization trials**

513 Subsets of mycorrhized roots were stained⁴¹ and quantified for their level of colonization
514 using the gridline intersect method⁴². Only the presence of clear intraradical structures
515 such as coiled cortical hyphae, arbuscles and vesicles were scored as positively
516 mycorrhized. A minimum of 200 intersecting root fragments per sample were
517 investigated microscopically for intraradical AM structures. For trials involving
518 W115xW1138 lines 5 individuals of 5 lines were analysed and the data presented as a
519 pool of N=25 (5x5). Double staining of colonized roots with propidium iodide and wheat
520 germ agglutinin coupled to fluorescein isothiocyanate (WGA-FITC; Sigma-Aldrich) was
521 performed as described⁴³.

522

523 **8 Hyphal branching bioassays**

524 Branching assays were performed as previously described⁴⁴ with pre-selected spores of
525 *Gigaspora margarita* (AGRAUXINE, France). For production of the root exudates
526 concentrate, petunia lines were grown in clay granules and were transferred for 24 h to
527 0.1 L of a hydroponic solution containing 2 mM CaCl₂ and 2 mM KSO₄ and kept under
528 constant aeration. The hydroponic solution was then run through a Sep-Pak Classic C18
529 Cartridge (Waters, Ireland) to adsorb hydrophobic root exudates. Exudates were eluted
530 from the column using 2 ml of acetone and the eluent was dried over nitrogen. Dried
531 exudates were re-dissolved in acetone and normalized according to root fresh weight
532 (FW). Exudate equivalents of 10 mg root FW were used in each branching assay.

533

534 **9 Transport assays and GR24 tolerance assays**

535 Arabidopsis seeds of three independent *PDR1*-OE lines were surface-sterilized with 1%
536 [v/v] bleach and 50% [v/v] ethanol and plated on media supplemented with 2.2 g L⁻¹ MS,
537 1% [w/v] sucrose and 0, 10, or 25 μM GR24. After three days of stratification plants
538 were moved to a 16 h light /8 h dark regime and selected for GFP fluorescence after 3
539 days of growth. Root length was determined with the ImageJ 1.44 software
540 (<http://rsbweb.nih.gov/ij>) after seven days and seedlings were moved to hygromycin-
541 containing plates without sucrose to confirm the selection by GFP fluorescence.

542 For transport experiments, seeds were sterilized in the same way and plated on
543 hygromycin-containing media. After three days of stratification and three days of growth,
544 seedlings were checked for GFP fluorescence. After seven days, GFP- and hygromycin-
545 positive plants were transferred to media supplemented with 2.2 g L⁻¹ MS, 1% [w/v]
546 sucrose and grown for another seven days. Three *PDR1*-OE lines, Col-0 and a vector
547 control line were incubated for 2 h in the dark at 4°C with root tips submerged in 0.1%
548 [w/v] Phytoagar (Duchefa Biochemie, The Netherlands) supplemented with 25 nM ³H-
549 GR24 (specific activity 40 Ci mmol⁻¹, American Radiolabeled Chemicals, USA).
550 Subsequently, the plant roots were washed in ice-cold 1 mM CaCl₂ and incubated in 200
551 μl 0.1% Phytoagar. For each line, 50% of the plants were further kept for 1 h at 4°C in
552 the dark as diffusion control, the other 50% were shifted for 1 h to 23°C to monitor
553 transport. Subsequently, shoot, root and Phytoagar fractions were incubated for 30 min in
554 50 μl 24% [w/v] trichloroacetic acid at 23°C. Tritium counts were determined in 3 ml

555 Ultima Gold LSC cocktail (Perkin Elmer, USA) with Liquid Scintillation Analyzer Tri-
556 Carb 2900TR (Packard BioScience, USA). Disintegrations per minute (dpm's) were
557 computed into percentages for each fraction and normalized to tissue fresh weights.

558

559

560 **10 RNA isolation, cDNA synthesis, semi-quantitative PCR and quantitative RT-** 561 **PCR**

562 RNA was isolated with the RNeasy Plant Mini Kit (Qiagen, Germany). Reverse
563 transcription of RNA to cDNA was performed with the M-MLV reverse transcriptase
564 (Promega, USA) and a polyT primer (Promega, USA).

565 *PhPDR1* expression was quantified semi-quantitatively with 5'-gaaactgtggccgaaagg and
566 5'-gagttcaagccggctct or 5'-aaatgtactacagtgcag and 5'-catataatgtccaggaaatggg. Tubulin1
567 transcript (*PhTUB*), partially amplified with 5'-cattggtcaagccggttattc and 5'-
568 acccttgaagaccagtacagt served as housekeeping and loading control.

569 Samples were diluted 1:30, and 4µl of the dilutions were added to each reaction well,
570 serving as template for the reaction. Deionized water served as negative control for
571 amplification. *PhPDR1* expression was quantified with 5'-cctgaggtttaccaaagg and
572 5'-gatggtattggattggagca. *Glyceraldehyde 3-phosphate dehydrogenase (GapDH)* expression
573 was quantified with 5'-gactggagaggtggaagagc and 5'-ccgtaagagctgggagaac. *GapDH*
574 served as housekeeping gene for normalization because it was shown to be not regulated
575 by hormonal treatments or mycorrhization (Didier Reinhardt, personal communication).

576 Final primer concentrations of 50, 100, 200, and 300 nM were tested for cDNA
577 amplification and melting behaviour in a range of 60°C – 95°C. Because no differences
578 were recorded, the average concentration of 100 nM was chosen for further experiments.
579 Primer efficiency was recorded with W115 root cDNA as template in a dilution range of
580 1:1 – 1:512, resulting in 94.42% for *PhPDR1* and 98.561% for *GapDH*. These values
581 were taken into account in the calculations. Sybr Green PCR Master Mix (Applied
582 Biosystems) was added to the samples to a final volume of 20 µl. For each sample, three
583 technical replicates were pipetted. RT-PCR was performed on a 7500 Fast Real-Time
584 PCR System (Applied Biosystems) with the 7500 Software v2.0.4. The Quantitation-
585 Comparative CT ($\Delta\Delta CT$) was chosen as method⁴⁵, the PCR run was divided into three

586 parts: 1. Hold stage (50°C for 2 min, 95°C for 10 min); 2. Cycling stage (95°C 15 s, 60°C
587 1 min for 40 cycles); Melt Curve stage (95°C 15 s, 60°C to 95°C 1 min, 95°C 30 s, 60°C
588 15 s). Relative differences were calculated as described^{45,46}. Each experiment was
589 performed for three biological replicates.

590

591 **11 Isolation, identification and quantification of petunia strigolactones**

592 Plants were grown in a X-stream 20 aeroponic system (Nutriculture, UK) as previously
593 described for *Medicago truncatula*⁴⁷. From day eight until day twelve exudates were
594 collected, pooled and root material sampled and stored at -80°C for further analysis. *P.*
595 *hybrida* root exudates and extracts were prepared and analyzed by ultra performance
596 liquid chromatography coupled to tandem mass spectrometry (UPLC-MS/MS) as
597 previously described for Arabidopsis²². Orobanchol was kindly provided by Koichi
598 Yoneyama (Weed Science Center, Utsunomiya University, Japan). For trials involving
599 W115xW1138 lines 3 individuals of 3 lines were analyzed and the data presented as a
600 pool of N = 9 (3x3).

601

602

603 **12 *Phelipanche ramosa* germination bioassay**

604 Germination assays with *P. ramosa* seeds were conducted as reported previously¹⁰.
605 Exudates were prepared as in 8. GR24 at 1 and 0.1 nM and demineralised water were
606 included as positive and negative controls. *P. ramosa* seeds were kindly provided by
607 Maurizio Vurro (Istituto di Scienze delle Produzioni Alimentari, Italy). For trials
608 involving W115xW1138 lines 2 individuals of 5 lines were analyzed and the data
609 presented as a pool of N = 10 (5x2).

610

611 **13 Trypan blue staining of hypodermal passage cells**

612 Trypan blue stains of hypodermal passage cells in roots were performed as described¹⁸.

613

614 **14 Axillary branching trials**

615 For a comparative analysis of lateral branch production in wild type and *pdr1*
616 backgrounds, plants were grown for 65 d in 0.55 L pots in soil as described in 1 and

617 watered daily. Branch development was monitored at different time points in a binomial
618 fashion (yes/no) in respect to the following parameters: bud length > 7 mm; full branch.
619 Full branches were scored in accordance to a petunia branch definition⁴⁸. Furthermore
620 branch length was scored as a continuous parameter. For trials involving W115xW1138
621 22 individuals of 5 lines were analyzed and the data presented as a pool of N = 110
622 (5x22). For branch length trials in response to GR24 treatments three lines each of
623 W115xW135, W115xW138-*pdr1*, V26, and *dad1* (kind gift of Kimberly Snowden, New
624 Zealand Institute for Plant and Food Research Limited, Auckland) were grown on soil as
625 described in **1**. From 25 - 40 dpv, plants were treated three times each week with 0 μ M or
626 10 μ M GR24 as described⁶. For trials involving W115xW1138 lines 8 individuals of 3
627 lines were analyzed and the data presented as a pool of N = 24 (3x8).

628

629 **15 Statistical analyses**

630 Depending on experimental set-ups and prerequisites Students t-tests, Fishers Exact tests
631 or generalized linear models (GLM) with quasi-binomial error structures were applied
632 using the “R” software (R Development Core Team 2009).

633

634 **16 Bioinformatics**

635 Analysis of DNA fragments and vector constructs was performed using VectorNTI
636 (Invitrogen). Membrane topology of PhPDR1 was predicted using ConPredII
637 (bioinfo.si.hirosaki-u.ac.jp/~ConPred2/). Phylogenetic analysis of PhPDR1 was
638 performed using tools available at phylogeny.fr (www.phylogeny.fr). Alignments were
639 performed with Multalin (multalin.toulouse.inra.fr/multalin/).

640

641 **17 Robustness of data sets**

642 All data sets presented were confirmed in at least two independent trials with similar set-
643 ups and outcomes. For mycorrhization and branching trials individual pots were
644 randomized to reduce positional effects and sample size was kept high to reduce
645 background effects.

646

647

648 **References:**

649

- 650 31. Zhang, X., Nakamura, I. & Mii, M. Molecular Evidence for Progenitorial Species
651 of Garden Petunias Using Polymerase Chain Reaction-Restriction Fragment
652 Length Polymorphism Analysis of the Chs-j Gene *HortScience* **43** 300-303
653 (2008).
- 654 32. Meyer, A., Eskandari, S., Grallath, S. & Rentsch, D. AtGAT1, a high affinity
655 transporter for γ -aminobutyric acid in *Arabidopsis thaliana*. *Journal of Biological*
656 *Chemistry* **281** 7197-7204 (2006).
- 657 33. Hellens, R. P., Edwards, E. A., Leyland, N. R., Bean, S. & Mullineaux, P. M.
658 pGreen: a versatile and flexible binary Ti vector for *Agrobacterium*-mediated
659 plant transformation. *Plant Mol Biol* **42**, 819-832 (2000).
- 660 34. Becker, D., Kemper, E., Schell, J. & Masterson, R. New plant binary vectors with
661 selectable markers located proximal to the left T-DNA border. *Plant Mol Biol* **20**,
662 1195-1197 (1992).
- 663 35. Cervera, M. Histochemical and fluorometric assays for uidA (GUS) gene
664 detection. *Transgenic Plants: Methods and Protocols* **286**. 203-213 (2004).
- 665 36. Wesley, S. V. et al. Construct design for efficient, effective and high-throughput
666 gene silencing in plants. *Plant J* **27**, 581-590 (2001).
- 667 37. Lutke, W. K. *Petunia* (*Petunia hybrida*). *Methods Mol Biol* **344**, 339-349 (2006).
- 668 38. Harrison, S. et al. A rapid and robust method of identifying transformed
669 *Arabidopsis thaliana* seedlings following floral dip transformation. *Plant Methods*
670 **2**, 19 (2006).
- 671 39. Vandenbussche, M. & Gerats, T. TE-based mutagenesis systems in plants: a gene
672 family approach. *Methods Mol Biol* **260**, 115-127 (2004).
- 673 40. Van den Broeck, D. et al. Transposon Display identifies individual transposable
674 elements in high copy number lines. *Plant J* **13**, 121-129 (1998).
- 675 41. Vierheilig, H., Coughlan, A., Wyss, U. & Piche, Y. Ink and vinegar, a simple
676 staining technique for arbuscular-mycorrhizal fungi. *Appl Environ Microbiol* **64**,
677 5004-5007 (1998).
- 678 42. Giovannetti, M. & Mosse, B. An Evaluation of Techniques for Measuring
679 Vesicular Arbuscular Mycorrhizal Infection in Roots. *New Phytologist* **84**, 489-
680 500.
- 681 43. Feddermann, N. et al. The PAM1 gene of *petunia*, required for intracellular
682 accommodation and morphogenesis of arbuscular mycorrhizal fungi, encodes a
683 homologue of VAPYRIN. *Plant J* **64**, 470-481 (2010).
- 684 44. Nagahashi, G. & Douds, D. D. Rapid and sensitive bioassay to study signals
685 between root exudates and arbuscular mycorrhizal fungi. *Biotechnology*
686 *Techniques* **13**, 893-897 (1999).
- 687 45. Livak, K. J. & Schmittgen, T. D. Analysis of relative gene expression data using
688 real-time quantitative PCR and the 2(-Delta Delta C(T)) Method. *Methods* **25**,
689 402-408 (2001).
- 690 46. Yuan, J. S., Reed, A., Chen, F. & Stewart, C. N. Statistical analysis of real-time
691 PCR data. *BMC Bioinformatics* **7**, 85 (2006).

- 692 47. Liu W. et al. Strigolactone biosynthesis requires the symbiotic GRAS-TYPE
693 transcription NSP1 and NSP2. *Plant Cell* (2011) [epub ahead of print, doi:
694 10.1105/tpc.111.089771]
- 695 48. Snowden, K. C. & Napoli, C. A. A quantitative study of lateral branching in
696 petunia. *Functional Plant Biology* **30**, 987-994 (2003/01/01).
697
698
699
700
701
702
703
704
705
706

Figure 1

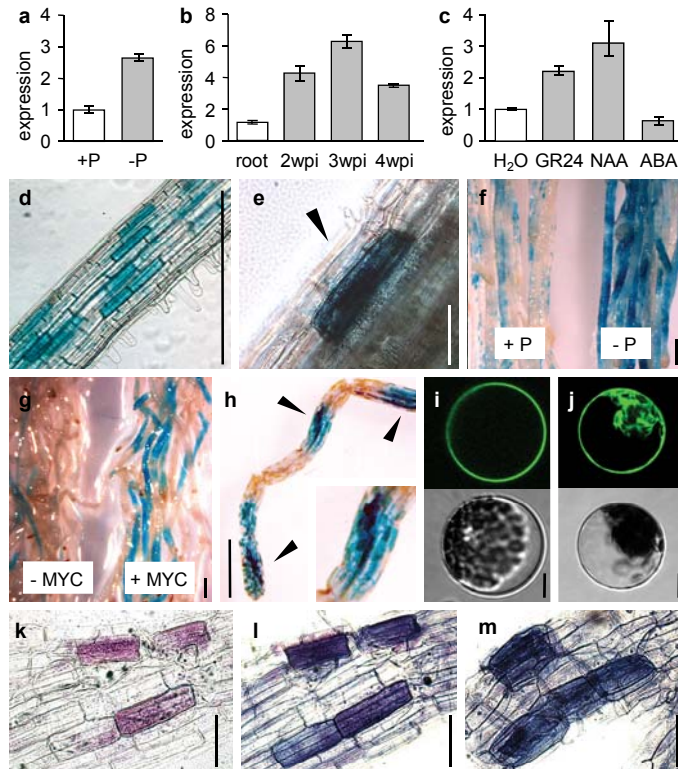


Figure 4

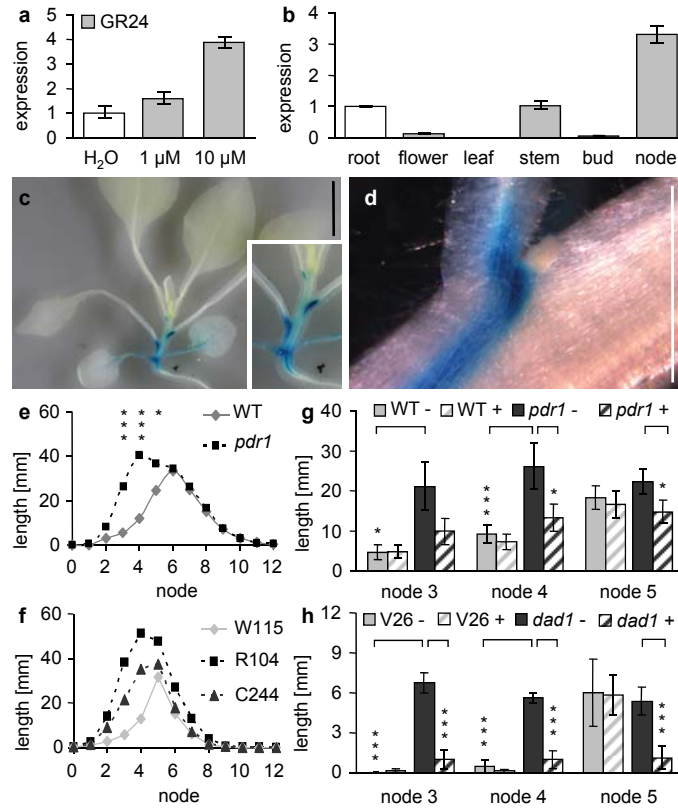


Figure 2

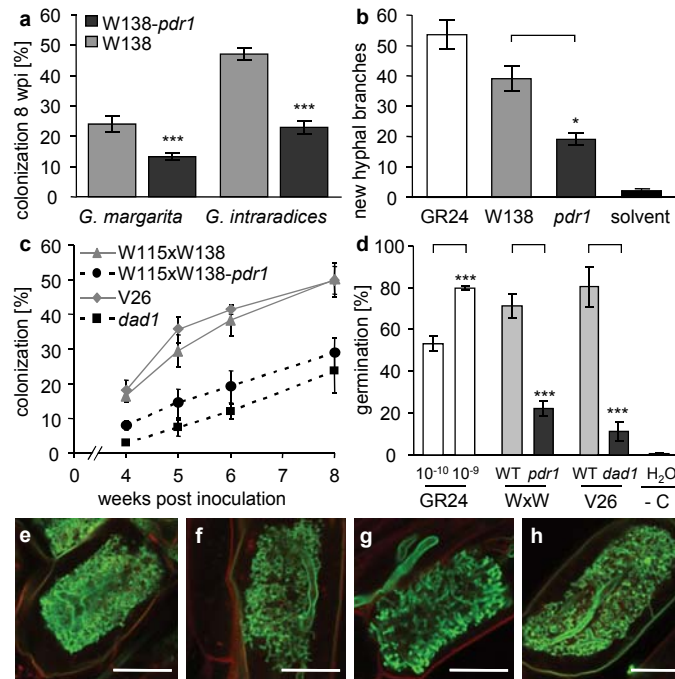


Figure 3

